Available online at www.sciencedirect.com
ScienceDirect
International Journal of Mass Spectrometry 269 (2008) 85–94
International Journal of Mass Spectrometry
www.elsevier.com/locate/ijms

Analysis of metastable ions in the ToF-SIMS spectra of polymers

A.G. Shard *, I.S. Gilmore

National Physical Laboratory, Teddington, Middlesex TW11 0LW, UK

Received 16 August 2007; received in revised form 19 September 2007; accepted 19 September 2007
Available online 29 September 2007

Abstract

This paper describes a simplified method to determine the parent and daughter ions of metastable peaks observed using a single stage reflectron ToF-SIMS instrument. The method requires two or more spectra, acquired with different reflector potentials and relies on the use of the apparent mass of the metastable, rather than the time-of-flight required by previous methods. We demonstrate the origin of metastable peak shapes, which depend upon the mass ratio of daughter and parent ions, the kinetic energy released during the decay process and the kinetics of the decay process. We highlight the difficulty of obtaining information from these shapes. The metastables of four common polymers, poly(ethyleneoxide), poly(lactide), poly(methylmethacrylate) and poly(tetrafluoroethylene) are used to provide comprehensive maps of the important in-flight fragmentation reactions. These maps demonstrate that the polymer structure is generally retained for high mass ions and the origin of the $C_4H_9O_2^+$ secondary ion in poly(lactide), a prominent but puzzling ion, is explained.

Keywords: Surface analysis; Secondary ion mass spectrometry

1. Introduction

The appearance of metastable ions in the ToF-SIMS spectra of polymers is well documented [1–4], yet their importance in spectral interpretation is often not fully appreciated. Whilst the appearance of metastable peaks in a ToF-SIMS spectrum can lead to misattributions if the metastable origin is not recognised, correct assignment of these ions can lead to a greater understanding of the molecular structure of the secondary parent ion and consequently a more detailed understanding of the surface. If the mass of the parent (or precursor) and daughter (or product) ions can be easily determined then the structural link between the two is provided by the presence of a metastable ion. Within a ToF analyser, it is possible to identify metastable peaks by altering the reflector voltage and observing a shift in arrival time of the metastable peaks relative to that of stable ions [1,2]. In Fig. 1 a peak appearing close to the position expected for the Al^+ stable ion with optimal instrumental settings is actually a metastable peak of molecular origin. This example also demonstrates that metastable peaks may be quite sharp, which leads to easy misidentification. In the high mass region of a ToF mass spectrum, metastable peaks become very important. This is mainly because of the long flight times of heavy ions, providing ample opportunity for decay processes to occur. An example is shown in Fig. 2, in which the majority of intensity arises from metastable peaks. With a reflector potential of 20 V, the high intensity of the metastable peaks obscures a weaker signal from ions that have not fragmented during flight. In this example, a weak metastable peak due to a double decay is also observed. It is possible to observe instances in which the parent ion of an observable metastable peak is, itself, not detectable due to complete decay during flight. The $(n\mathrm{M}-\mathrm{O})^{\bullet+}$ series for poly(lactide) with $n>6$ provide such examples, for our instrument and settings. Misidentification of metastable peaks in the high mass region is likely because mass accuracy is often insufficient to reliably identify stable ions. The unintentional inclusion of metastable peak intensities will cause problems in quantitative analysis and it is therefore important to be able to identify such peaks.

Within this paper we describe a straightforward method to elucidate the parent and daughter masses from the apparent mass of the metastable ion. The approach requires that two or more spectra be acquired from the sample using different reflector potentials. We also show how the shape of the metastable peak is related to the parent and daughter masses and the lifetime of the parent ion. Finally we demonstrate the utility of metastable

* Corresponding author. Tel.: +44 208 943 6193.
E-mail address: alex.shard@npl.co.uk (A.G. Shard).

1387-3806/$ – see front matter.
doi:10.1016/j.ijms.2007.09.011

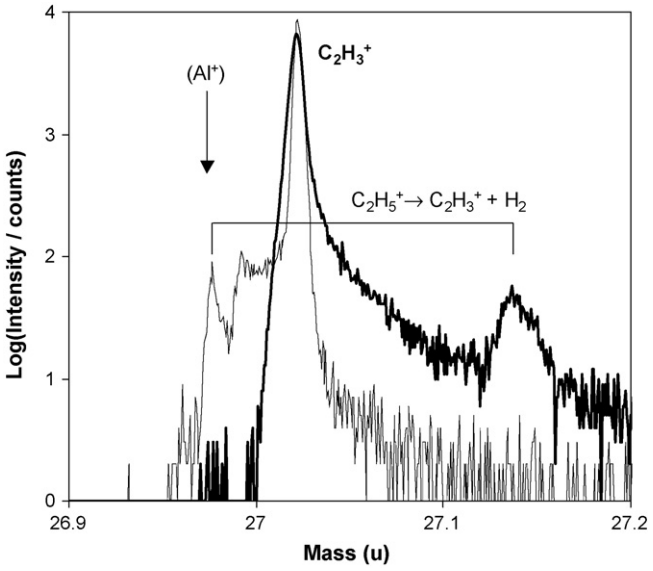

Fig. 1. Example of a sharp metastable peak which could be easily misidentified as Al^+. Overlay of ToF-SIMS spectra of the 27 u region of poly(ethyleneoxide) taken with reflector potentials of 20 V and 400 V (bold).

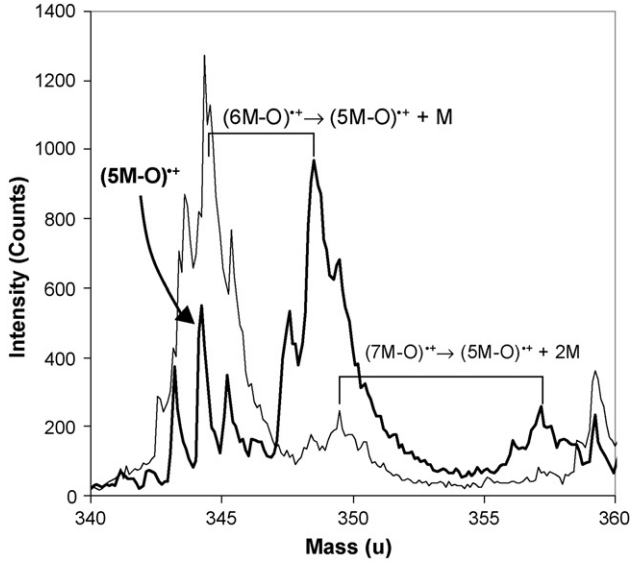

Fig. 2. Example of spectra in which metastable peaks have dominant intensity: overlay of ToF-SIMS spectra of the $(5M-O)^{\bullet+}$ region of poly(lactide) taken with reflector potentials of 20 V and 300 V (bold).

analysis in unravelling structural links between ions in the ToF-SIMS spectra of polymers.

2. Theory

2.1. The apparent mass of metastable ions in a reflectron ToF mass spectrometer

In a reflectron time-of-flight mass spectrometer an ion is rapidly accelerated in the extraction region and passes through an initial, field free, drift region of length, L_1, into an ion mirror of length, L_r, a second drift region of length L_2 before being accelerated into the detector. The initial and final acceleration can have a significant influence on the arrival time of the ion, however in our simple analysis we ignore these regions and demonstrate later how compensation can be made. We define a total drift length of $L_d = L_1 + L_2$ and, for an ion of mass m_i and drift region kinetic energy E_i, using a drift potential of $-V_d$ and a reflector potential of V_r the ion flight time, t_i, is given by Eq. (1), in which e is the charge on the ion.

$$t_i = \sqrt{2m_i}\left(\frac{\sqrt{E_i}}{e(V_r + V_d)}2L_r + \frac{1}{\sqrt{E_i}}\frac{L_d}{2}\right) \quad (1)$$

For ions that are stable throughout their flight, kinetic energy is given by $E_i = eV_d$ provided there is no charge accumulation or penetration of the extraction field at the sample surface. With similar constraints, a metastable ion that decays in the first drift region has $m_i = m_d$ and $E_i = eV_d m_d/m_p$, where m_d is the mass of the daughter ion and m_p is the mass of the parent ion. Equating the arrival time of the metastable with a putative stable ion that has the same flight time gives the apparent mass, m_a, of the metastable ion as shown in Eq. (2).

$$\sqrt{m_a}\left(V_r + V_d\left(1 + \frac{4L_r}{L_d}\right)\right) = \sqrt{m_p}V_r + \sqrt{m_p}V_d\left(1 + \frac{m_d}{m_p}\frac{4L_r}{L_d}\right) \quad (2)$$

The parent and daughter masses may be found by plotting the term on the LHS of Eq. (2) against V_r and extracting values for m_p and m_d from the slope and intercept of the resulting line. This method is essentially no different from previously published approaches [1,2], but has the advantage that it uses the apparent mass of the metastable, which will be a convenience for most analysts. If only two observations of apparent mass, m_1 and m_2, are available, taken with different reflector potentials, V_1 and V_2, then the rearrangement shown in Eq. (3) is useful following the substitution of $m_a = (m_1 + m_2)/2$, $V_r = (V_1 + V_2)/2$ and $dm_a/dV_r \approx (m_2 - m_1)/(V_2 - V_1)$. The daughter mass can then be found straightforwardly from Eq. (2).

$$\sqrt{m_p} = \frac{1}{2\sqrt{m_a}}\left(V_r + V_d\left(1 + \frac{4L_r}{L_d}\right)\right)\frac{dm_a}{dV_r} + \sqrt{m_a} \quad (3)$$

The length ratio, $4L_r/L_d$ for the spectrometer needs to be determined and should be a number close to unity, as can be demonstrated by taking the differential of Eq. (1) with respect to kinetic energy:

$$\frac{dt}{dE_i} = \sqrt{2m_i}\left[\frac{L_r}{e(V_r + V_d)}(E_i)^{-0.5} - \frac{L_d}{4}(E_i)^{-1.5}\right] \quad (4)$$

The purpose of a reflectron instrument is to decouple the arrival time from the kinetic energy distribution arising from the emission process. This is achieved when Eq. (4) is equal to zero, the condition for which is shown in Eq. (5).

$$\frac{4L_r}{L_d} = \frac{e(V_r + V_d)}{E_i} \quad (5)$$

In general $V_d \gg V_r$, and for stable ions the condition is best met with a length ratio slightly greater than unity. However, for

metastable ions the ideal drift length is shorter by a factor m_d/m_p, a point that will be returned to when discussing metastable peak shapes. It was noted earlier that acceleration during extraction and detection is neglected in this treatment. Eq. (6), in which L_x is the length and $-\Delta V_x$ the potential difference across the accelerating region x, shows the additional flight time, Δt_x, which should be added to Eq. (1) for each region. The term $E_{i,x}$ represents the kinetic energy of the ion prior to acceleration and for the extraction region should be close to zero.

$$\Delta t_x = \frac{\sqrt{2m_i}L_x}{e\,\Delta V_x}\left[\sqrt{e\,\Delta V_x + E_{i,x}} - \sqrt{E_{i,x}}\right] \quad (6)$$

By including these additional times, the resulting expression for apparent mass is unwieldy; however the form of Eq. (6) has similarities to the expression for flight time through the reflector within Eq. (1) and we find that in practice it is possible to use Eq. (2) to determine parent and daughter masses after minor adjustments to the values of V_d and $4L_r/L_d$ have been made. This is best done by identifying metastable peaks for which the parent and daughter masses are easily determined and altering the values to fit. Since this is an instrumental effect, these values only need to be determined once for a given drift potential. Following this procedure the typical uncertainty in the determination of the parent mass is <1% and <0.5% for the daughter mass. This is a comparable uncertainty to that described previously by L'Hermite et al. [2], in which the extraction region was taken into account but the probably more significant detection region was not. Inclusion of terms for acceleration during extraction and detection, shown in Eq. (6), reduces the uncertainty by more than a factor of two for both parent and daughter masses.

2.2. Metastable peak shapes in a reflectron ToF mass spectrometer

The shape of a metastable peak in a time-of-flight mass spectrometer depends upon the ratio of daughter mass to parent mass, the kinetic energy distribution of daughter ions from the decay process and the lifetime of the metastable ion. The initial kinetic energy distribution of the parent ion is less important than that induced by the decay process purely because the decay occurs post-extraction. Elementary considerations show that an event that results in an kinetic energy spread of ions, δE, from a parent that is stationary in the laboratory frame will, post-extraction, generate an energy spread, δE^*, given by Eq. (7) to a first order

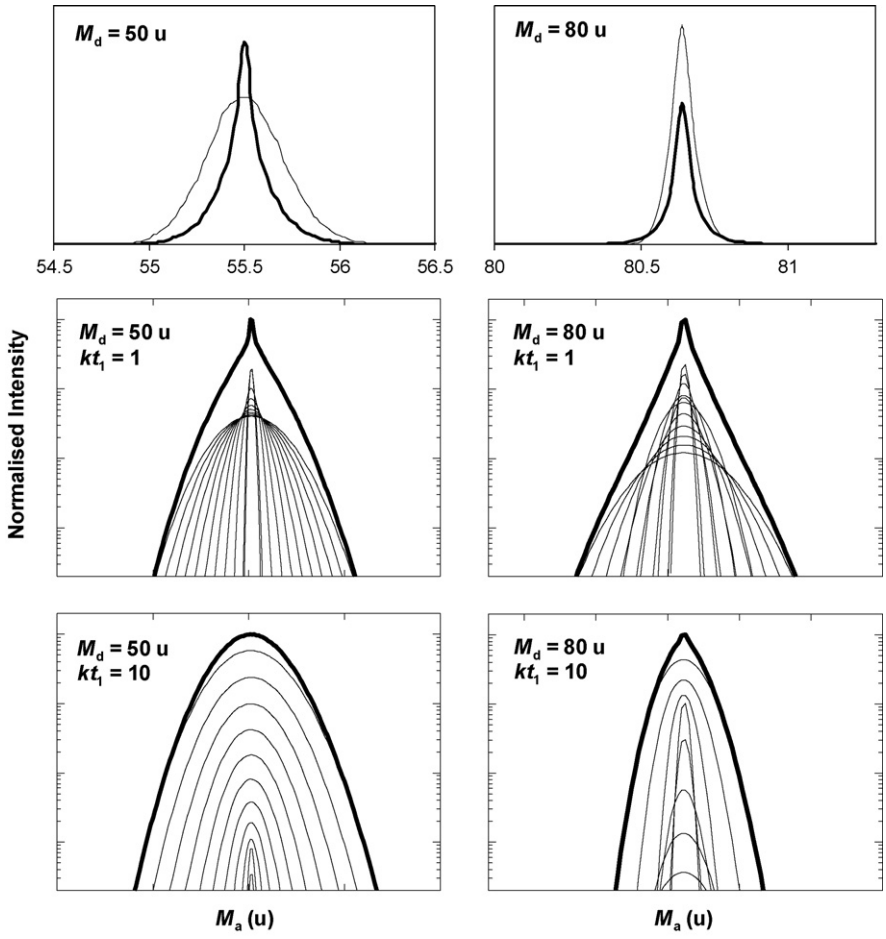

Fig. 3. Simulation of metastable peak shapes in a simplified reflectron instrument with $V_r = 20$V, $V_d = 2090$ V, $4L_r/L_d = 1.095$ and $m_p = 100$ u. The shapes for slowly decaying ions ($kt_1 = 1$) are shown in bold along with the shapes for rapidly decaying ions ($kt_1 = 10$). In the lower figures, contributions from decays at discrete points evenly spaced along the flight path, L_1, are shown in semi-logarithmic plots, demonstrating how the daughter to parent mass ratio and the decay kinetics alter the overall peak shape.

approximation.

$$\delta E^* = 2\sqrt{E_i\,\delta E} \tag{7}$$

Thus, with a drift kinetic energy of 2 keV, a post-extraction decay that would result in a 10 meV kinetic energy spread prior to extraction actually produces a ~9 eV kinetic energy spread. In the following, we ignore the effect of the pre-extraction secondary ion kinetic energy distribution (typically ~2 eV) on the peak shape and focus on the effect of kinetic energy imparted to the daughter ion in the decay process. The distribution function of velocities in the direction of flight, and therefore arrival times, from a post-extraction decay is assumed to be approximately Gaussian. However, the width of the time-of-flight distribution function depends upon the position of the decay within the flight length L_1, as suggested by Eq. (4), and will increase linearly with distance from the ideal drift length found from Eq. (5). The intensity contribution at each position in the flight path will depend upon the initial parent intensity and the kinetics of the decay process.

We now simulate metastable peak shapes using the simple reflectron model of Eq. (1), with $L_1 = L_2$ and using values of $4L_r/L_d = 1.05$ to take approximate account of the acceleration regions not in the model. We assume that the metastable parent decay is first order, with rate constant, k, given in units of t_1^{-1}, where t_1 is the time-of-flight for the ion through L_1. In addition, we assume that that the metastable daughter ion has a Gaussian velocity distribution for the decay (Eq. (8)), where v_x is the velocity change in the direction of flight and f the normalised distribution function) with $\delta E = 0.05$ eV. The calculated metastable peak shapes for decays at even time intervals in the first drift region, together with the overall peak shapes are shown in Fig. 3. It is clear that the peak shape, for ions with $kt_1 < 1$, is not well approximated by a Gaussian curve, which was previously suggested [5].

$$f = \sqrt{\frac{m_i}{4\pi\,\delta E}}\,\exp\left(\frac{-m_i v_x^2}{4\,\delta E}\right) \tag{8}$$

For metastables with $kt_1 < 1$ the peak shape in the time domain is approximated by the summation of Gaussian distributions in Eq. (9) in which I is the total integrated intensity and t_0 is the mean arrival times of metastable ions. The Gaussian is constrained to have constant area, representing a constant production rate throughout parent flight and the standard deviation of the curve is given by τ. This integral cannot be evaluated analytically and the curve is crudely approximated in Eq. (9) by a rectangular function of width 2τ, demonstrating that the peak shape for long-lived metastables will approximate to a symmetrical logarithmic decay. This approximation is equivalent to assuming that all daughter ions have the same velocity change upon decay, isotropically distributed with respect to the flight direction. A similar distribution of metastable arrival times is found in linear time-of-flight spectrometers using this approx-

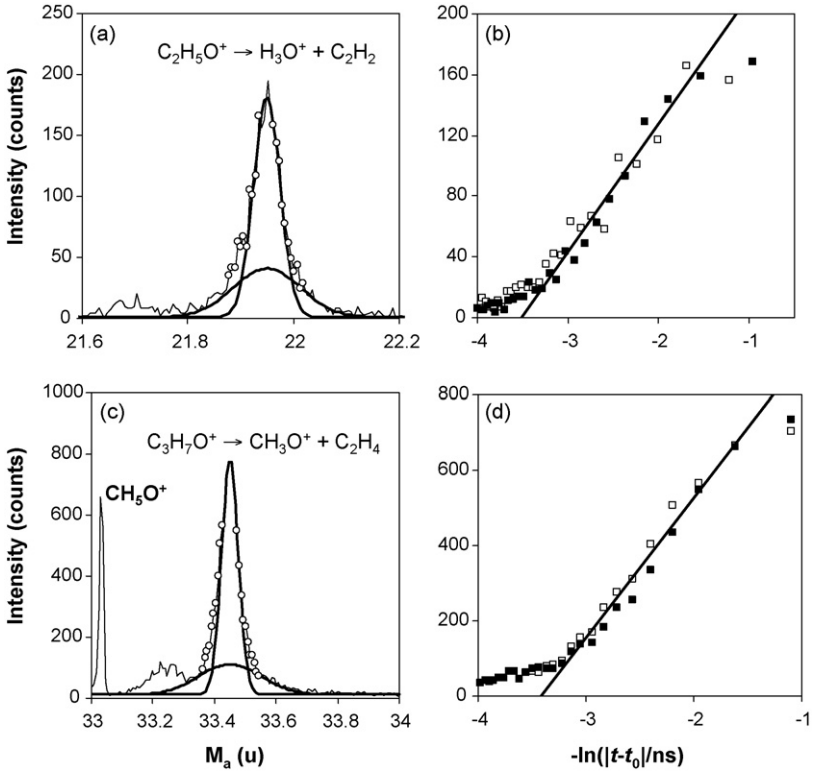

Fig. 4. Metastable ions observed in PEO: (a) and (c) show raw data, points which are marked (◯) are used in (b) and (d) respectively to provide a linear fit. Data points at lower apparent mass than the peak (□) are distinguished from those at higher apparent mass (■), but no distinction is made for the linear fit. These fits provide $\tau_{max} \approx 33$ ns and $\delta E \approx 35$ meV for (a, b) and $\tau_{max} \approx 28$ ns and $\delta E \approx 36$ meV for (c, d). The broad Gaussian curves of width τ_{max} in (a and c) demonstrate a good fit to the tail of the peaks, a narrower Gaussian curve is shown to describe the apex of the peak rather well ($\tau = 9$ ns for (a) and $\tau = 8$ ns for (c)) but not the overall peak shape.

imation as an assumption [6]. The approximation is not valid when t approaches t_0 and the peak shape in this region will be dominated by other factors, such as the initial kinetic energy distribution and instrumental resolution. It is also not valid when $|t - t_0|$ approaches τ_{max}, the maximum standard deviation of the Gaussian distribution, which can be approximated from Eqs. (4), (5) and (7) and shown in Eq. (10) for an ideal setting of V_r. Additionally, the expression is only valid for decays occurring from the start of L_1 to the optimal focus position suggested by Eq. (5) and assumes that this position occurs within L_1. It is therefore possible to extract the approximate kinetic energy release from metastable decompositions using the metastable peak shape as shown in Fig. 4, but the analysis is generally not trivial. It should also be noted that the peak shape and intensity is influenced by the efficiency of detection, bearing in mind the flight path of the metastable.

$$I_t = \frac{I}{\sqrt{2\pi}\tau_{max}} \int_0^{\tau_{max}} \frac{1}{\tau} \exp\left(\frac{-|t-t_0|^2}{2\tau^2}\right) d\tau \approx \frac{I}{2\tau_{max}} \int_{|t-t_0|}^{\tau_{max}} \tau^{-1} d\tau = N \ln\left(\frac{\tau_{max}}{|t-t_0|}\right) \quad (9)$$

$$\tau_{max} \approx \frac{dt}{dE_i} \delta E^* \approx \sqrt{\frac{m_d}{2}} L_d \left(\frac{1}{E_d} - \frac{1}{E_p}\right) \delta E^{0.5} = \sqrt{\frac{m_d}{2}} \frac{L_d}{eV_d} \left(\frac{m_p}{m_d} - 1\right) \delta E^{0.5} \quad (10)$$

Notwithstanding the difficulty involved in the analysis of metastable peak shapes, there are two important results that are of general interest: Firstly, the flight time at the metastable peak maximum intensity is accurately given by the time calculated in Eq. (1) even when broadening effects are taken into account. Secondly, for metastable peaks of similar daughter and parent masses an identical peak shape indicates identical decay kinetics and daughter kinetic energies, therefore an identical fragmentation process can be inferred. This second point has implications for structural assignments; in Fig. 2 the triplet of metastable peaks have identical shapes and their intensity ratios are the same as that of the stable parent ions, therefore the same fragmentation process occurs. The fragmentation reaction does not depend on the fact that one of these ions is a radical. If fragmentation occurs at the charge centre, as is commonly presumed, this is a strong argument in favour of the separation of the radical and charge centres within the radical cation (a distonic ion), as proposed previously [7].

3. Experimental

In this study, four polymers were used; poly(methylmethacrylate) (PMMA), poly(ethyleneoxide) (PEO), poly(lactide) (PLA) and poly(tetrafluoroethene) (PTFE). Thin films of PMMA, PEO and PLA were spin cast from appropriate solvents onto solvent-cleaned silicon wafers and allowed to dry prior to analysis. Analysis was performed on a TOFSIMS IV (IONTOF Gmbh, Münster, Germany) time-of-flight secondary ion mass spectrometer using a 10 keV Cs^+ primary ion source. Charge compensation using a low energy electron flood was only necessary in the case of PTFE. Typically, five spectra were acquired from separate 100 μm × 100 μm areas with a total primary ion dose of $<10^{12}$ ions m^{-2} and reflector potentials of V_r = 20 V, 100 V, 200 V, 300 V and 400 V, respectively. The drift potential was set to V_d = 2000 V in all cases. Spectra were also acquired using 10 keV Ar^+ ions as the primary source and G-SIMS analysis performed as described previously [8–10]. The data acquisition for PTFE has been described in an earlier work [1].

In order to use Eq. (2) for the general analysis of metastable ions, we must first determine appropriate values of V_d and $4L_r/L_d$ through calibration with known metastable decays, such as those from PTFE [1]. This provides values of V_d = 2090 V and $4L_r/L_d$ = 1.095. The drift potential and length ratio found in this manner do not represent real experimental parameters, but effective parameters for the simple model used to describe the flight time of ions. Metastable peaks were identified as those that increased in apparent mass as the reflector potential was increased; an example is shown in Fig. 5. Analysis of this metastable according to Eq. (2) returns m_p = 56.1 u and m_d = 27.9 u. With the inclusion of terms for the extraction and detection region shown in Eq. (6), the predicted masses with V_d = 2000 V are m_p = 55.9 u and m_d = 28.0 u. This metastable can therefore be identified as arising from the reaction $C_3H_4O^{\bullet+} \rightarrow C_2H_4^{\bullet+} + CO$. Further validation is provided by the observation that both parent and daughter are detected with strong intensity as stable ions; the possibility of $CO^{\bullet+}$ as the daughter ion was eliminated on this basis. Although it is not necessarily the case that detectable stable parent and daughter ions should accompany metastable peaks, it is reasonable to suppose that this should be true, particularly if the flight time is relatively short.

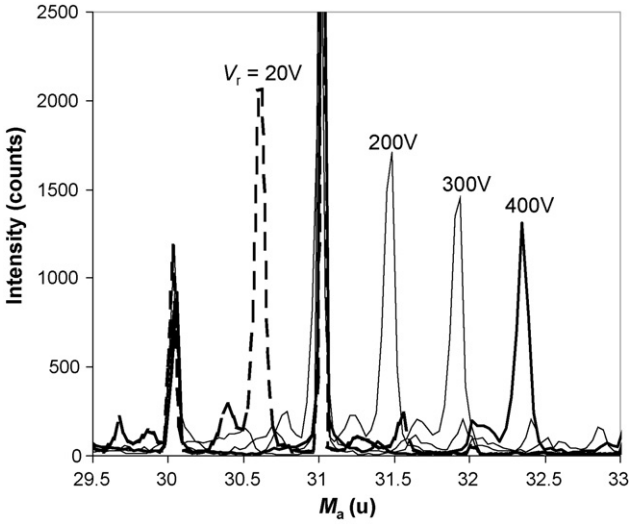

Fig. 5. Overlay of ToF-SIMS spectra of poly(lactide) taken with various reflector potentials, at V_r = 100 V the metastable peak overlaps the 31 u peak. The metastable shown here can be identified as arising from the reaction: $C_3H_4O^{\bullet+} \rightarrow C_2H_4^{\bullet+} + CO$.

4. Results

The peak positions of some of the metastable ions observed during SIMS of PEO are shown in Fig. 6a as a function of V_r. It is found that the dependence of m_a on V_r is close to linear over the range used here, as shown by the fits to the data. This shows that Eq. (3) may be used with only two data points to determine m_p, although the uncertainty is worse, typically 2%. The use of only two spectra to determine parent and daughter mass can also be problematic if one of the apparent mass positions is coincident with a stable ion or there are a number of metastable ions with similar apparent mass and intensity in the spectra. In the second case it can be difficult to reliably establish the connection between peaks in the two spectra. We recommend the use of at least four values of V_r to overcome these problems. Fig. 6b shows the analysis of the data in Fig. 6a according to Eq. (2). The important metastable decay pathways obtained in this manner for PEO are shown in Fig. 7. The metastable decay pathways are selected on the basis of whether the metastable are intense or whether either the parent or daughter is prominent within the G-SIMS spectra of the polymer. In some cases, there is more than one stable ion at the nominal mass of the parent or daughter and it is not possible to distinguish which ion is involved in the observed metastable decay. Often it is possible to eliminate one of the ions on the basis of chemical composition (for example, if the daughter ion contains an oxygen atom, then the parent ion must contain at least one oxygen atom). In the remaining cases of ambiguity, the most intense stable ion at the indicated nominal mass was selected. This provides the analyst with significantly more structural information than is available in the SIMS spectrum alone. Together with G-SIMS, it provides a powerful means to identify organic species.

The metastable decay pathways for PLA are shown in Fig. 8. There is a comparable intensity of stable ions from the $(n\mathrm{M}+\mathrm{H}-\mathrm{O})^+$ and $(n\mathrm{M}-\mathrm{CH_3})^+$ series at nominal mass $(72n-15)$ u for $n>1$ and also for the $C_5H_9O_2^+$ and $C_4H_5O_3^+$ ions at nominal mass 101 u. In these cases, it is not possible to determine which of the ions are responsible for the observed metastable peaks. There is therefore a degree of ambiguity in the assignment of some metastable peaks and the two possibilities are shown in the figure. Metastable peaks were observed to high mass, as demonstrated in Fig. 2, with the loss of one, two or even three monomer units during the decay. Since the intensity of metastable peaks associated with the loss of multiple monomer units increased with the mass of the parent ion, it is presumed that these arise from the sequential loss of single monomer units. Their observation at high mass is a consequence of the longer flight time of the parent ion giving the opportunity for sequential decays to occur.

A large number of metastable peaks were observed for PMMA, a selection is shown in the metastable decay pathways in Fig. 9. The metastable decay pathways that include either intense metastable peaks and/or stable ions identified by G-SIMS are shown. There are a large number of secondary ions with different compositions but the same nominal mass. This complicates the identification of parent and daughter ions. An example is shown in Fig. 9 of two ions with nominal mass 127 u, $C_6H_7O_3^+$ and $C_7H_{11}O_2^+$. The former ion is identified by G-SIMS as having undergone minimal fragmentation and should be more indicative of the polymer structure. Two of the metastable peaks that have a parent ion at 127 u have daughter ions which can be identified

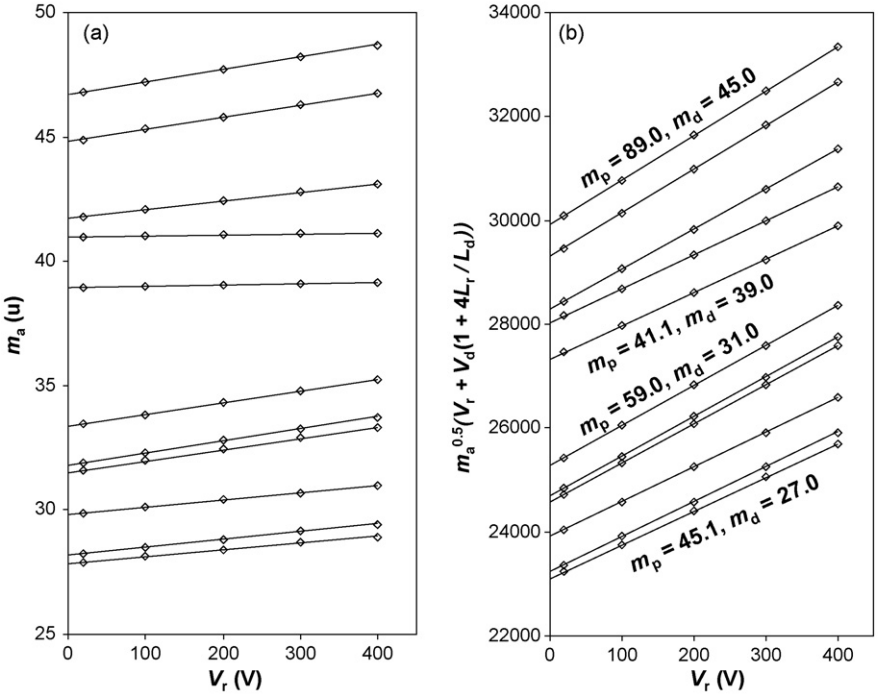

Fig. 6. Selected metastable ions observed in PEO plotted as a function of reflector potential against (a) apparent mass and (b) the LHS term of Eq. (2). Both graphs show linear fits to the data. Parent and daughter masses for four metastable ions, calculated from the slopes and intercepts in (b) are also shown.

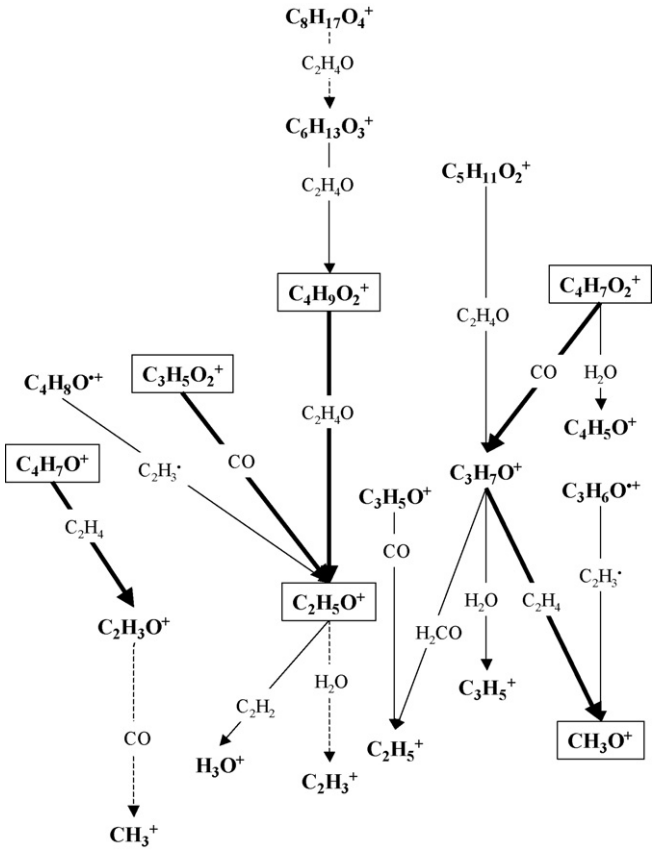

Fig. 7. The metastable decay pathways for PEO. Arrows connect parent ions to daughter ions with the presumed identity of the neutral fragment overlaid. Dashed arrows indicate integrated intensities of <1000 counts and bold arrows >10,000 counts for the metastable peak. Stable ions shown in boxes are prominent in the G-SIMS spectrum of the polymer.

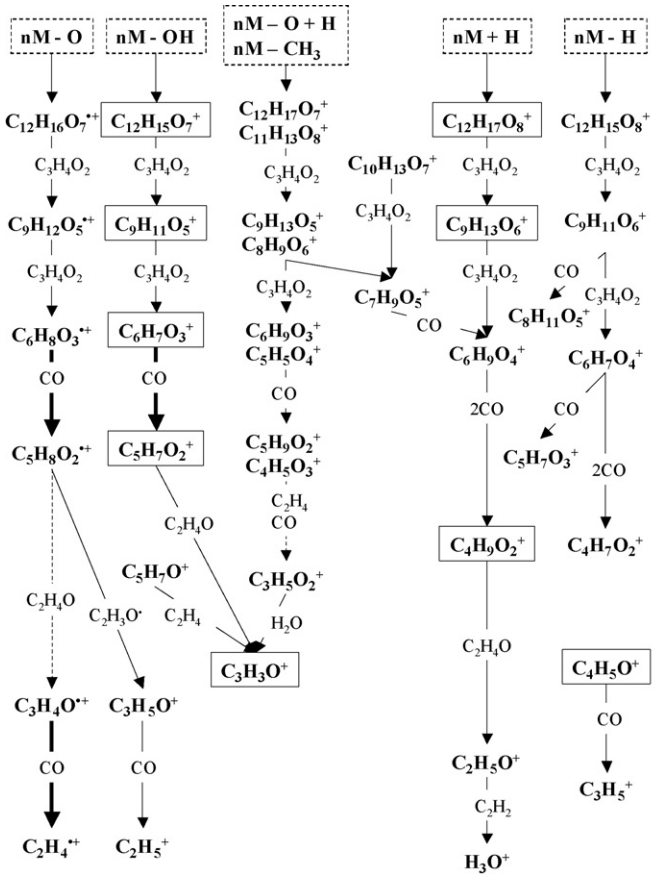

Fig. 8. The metastable decay pathways for PLA. Arrows connect parent ions to daughter ions with the presumed identity of the neutral fragment overlaid. Dashed arrows indicate integrated intensities of <1000 counts and bold arrows >10,000 counts for the metastable peak. Stable ions shown in boxes are prominent in the G-SIMS spectrum of the polymer. Dashed boxes indicate a series of metastable ions that continues to higher mass than shown in the diagram ($n > 4$).

as $C_6H_7O^+$ and $C_6H_7O_2^+$. These almost certainly arise from the latter ion, because otherwise the neutral fragments would be O_2 and O respectively, which seems unlikely. Another daughter, $C_5H_7O_2^+$, could have either ion as the parent.

The metastable decay pathways observed for PTFE, taken from previous data [1] are given in Fig. 10. The analysis in this case is straightforward, the only possible ambiguity being whether the observed loss of C_2F_4 as a neutral fragment from $C_6F_{11}^+$ and $C_5F_9^+$ is actually the sequential loss of two difluorocarbene ($:CF_2$) moieties. This is thought unlikely on the basis that related ions, such as $C_6F_9^+$ and $C_5F_7^+$ do not show the loss of C_2F_4 and the observation is likely to be of significance for structural interpretation.

5. Discussion

All of the polymer samples studied here display a wealth of metastable peaks during ToF-SIMS analysis. This is not limited to the examples given in this paper; metastable peaks are frequently observed in all ToF-SIMS spectra of organic materials provided that skimmers have not been fitted to the instrument to remove them [11]. The simple procedure described here, using a minimum of two spectra at different reflector potentials allows the metastable decay pathways to be identified. This provides a structural link between two stable ions, which aids both in the identification of species and the interpretation of ToF-SIMS data. For some polymers, such as PMMA, there are a large number of metastable peaks and it becomes particularly important to identify the structurally relevant parent and daughter ions in order to simplify the interpretation. G-SIMS has proven extremely useful in this regard. The metastable peaks are sometimes comparable in width and intensity to minor peaks in the ToF-SIMS spectra and, because their position will alter with experimental parameters, this could lead to problems with comparability of data between instruments and misidentification of trace contaminants.

One of the notable findings is that for the two polymers with heteroatoms in the main chain (PEO and PLA) the dominant neutral loss for high mass parent ions is the monomer unit. This implies that the secondary ions have retained the structure of the polymer and that a common decay mechanism exists for all ions that contain more than two monomer units. The structure of the most intense secondary ion from PEO ($C_2H_5O^+$) has been discussed previously [12] and either a linear or cyclic structure can be proposed for ions containing two or more monomer units. Given that the major fragmentation mechanism (loss of a single

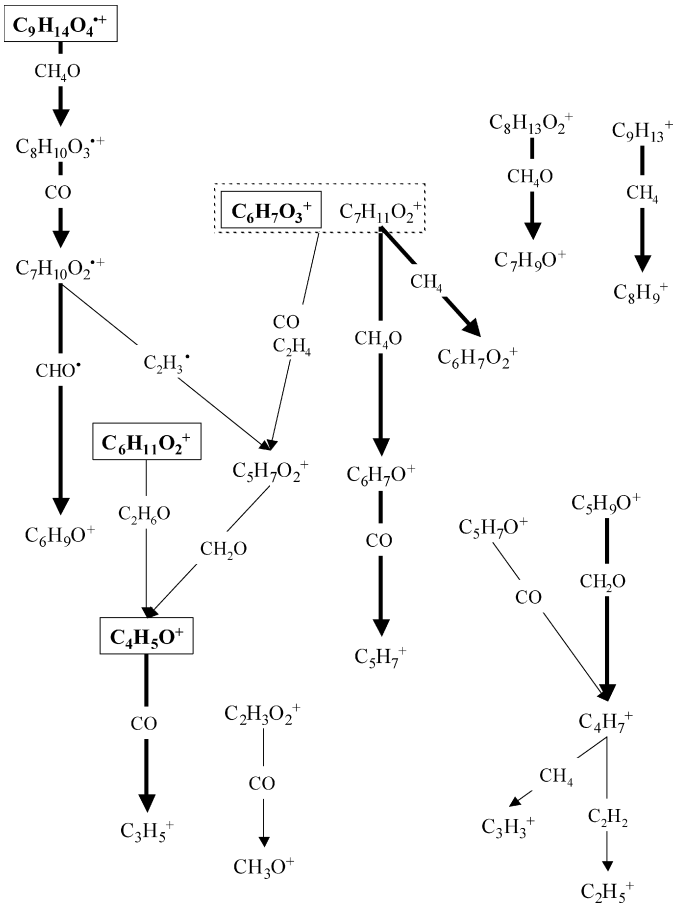

Fig. 9. The metastable decay pathways for PMMA. Arrows connect parent ions to daughter ions with the presumed identity of the neutral fragment overlaid. Dashed arrows indicate integrated intensities of <1000 counts and bold arrows >10,000 counts for the metastable peak. Stable ions shown in boxes are prominent in the G-SIMS spectrum of the polymer. The dashed box indicates two ions with nominal mass 127 u.

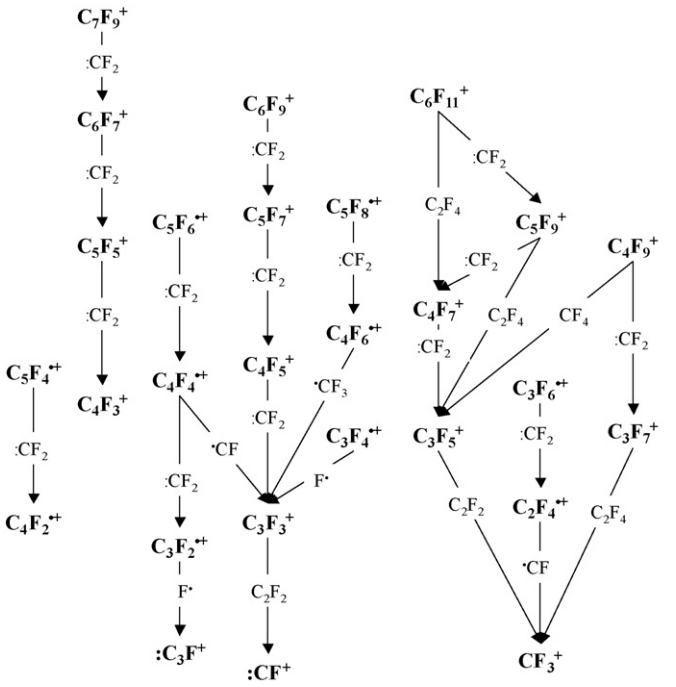

Fig. 10. The metastable decay pathways for PTFE. Arrows connect parent ions to daughter ions with the presumed identity of the neutral fragment overlaid.

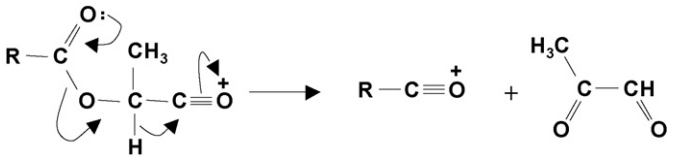

Scheme 2. Concerted mechanism for the loss of monomer ($C_3H_4O_2$) fragments from PLA secondary ions.

monomer unit) does not change, regardless of the number of monomer units, this strongly implies a linear structure for the ions. We speculatively propose a concerted mechanism for this process in Scheme 1.

For PLA, a similar, concerted mechanism for the loss of monomer units can be proposed as shown in Scheme 2, but a two-step mechanism that does not involve a hydride shift may be more likely. This is shown in Scheme 3. The sequence of CO and C_2H_4O neutral loss is drawn from the observation that this is the sequence observed for the $C_6H_7O_3^+$ and $C_6H_8O_3^{\bullet+}$ ions. In the case of PLA the loss of monomer units from secondary ions no longer occurs when the parent ion contains two monomer units or fewer atoms. The linear structure of high mass ions can be supported using entropic arguments; however, once the ion contains between one and two monomer units a cyclic structure may form and significantly alter the subsequent decay processes. The loss of two carbon monoxide neutral fragments from the $C_6H_9O_4^+$ $(2M+H)^+$ and $C_6H_7O_4^+$ $(2M-H)^+$ secondary ions are difficult to rationalise without invoking a cyclic intermediate. It is natural to assume that the precursor for the loss of carbon monoxide is the carbonyl group in the polyester. Following the loss of one carbon monoxide neutral fragment, the remaining precursor group for these ions is no longer at one of the ends of the molecule. Without a cyclic intermediate, the loss of carbon monoxide would therefore imply that the secondary ion has undergone scission into three parts, two of which have recombined during flight. Such a scheme is not credible. A plausible mechanism for the $C_6H_9O_4^+$ ion, involving a cyclic intermediate is outlined in Scheme 4. Because there is no detectable metastable from this ion associated with a single loss of CO and the observation that the intermediate (at nominal mass 117 u)

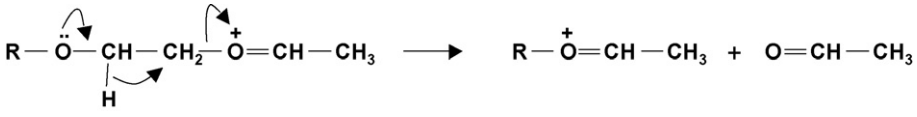

Scheme 1. Proposed mechanism for the loss of monomer (C_2H_4O) fragments from PEO secondary ions.

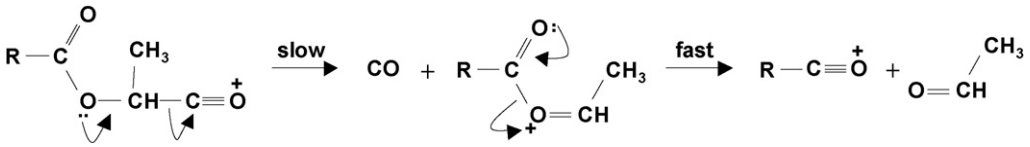

Scheme 3. Two-step mechanism for the loss of monomer ($C_3H_4O_2$) fragments from PLA secondary ions.

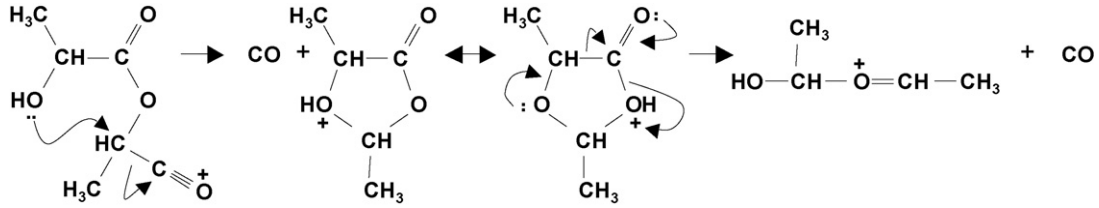

Scheme 4. Proposed mechanism for the loss of two carbon monoxide molecules from the $C_6H_9O_4^+$ ion.

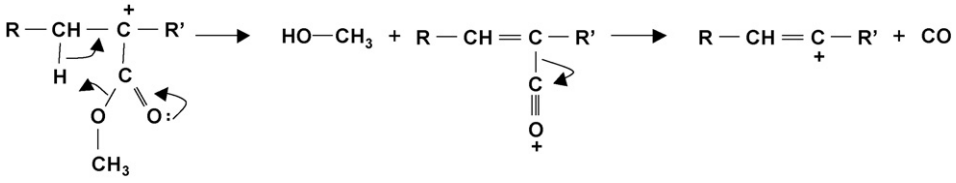

Scheme 5. Possible two-step mechanism for the loss of side groups in PMMA secondary ions.

is weak in intensity as a stable ion, the second step must be fast in comparison to the first step. The product of this decay, $C_4H_9O_2^+$, subsequently undergoes loss of C_2H_4O and it is easy to see that this is in accord with the proposed mechanism (cf. Schemes 1 and 3). The importance of this observation of double CO loss is twofold. Firstly, it explains the origin of the $C_4H_9O_2^+$ ion, which is difficult to rationalise from the structure of the polymer. Secondly, the intensity of the $(n\text{M+H})^+$ ion series has a strong dependence on the molecular weight of the polymer for $n > 1$ due to an enhanced yield from end-groups [13]. However, the $(\text{M+H})^+$ ion, $C_3H_5O_2^+$, does not show this effect, yet the $C_4H_9O_2^+$ secondary ion does. These observations from an independent study entirely support the findings here: the $(\text{M+H})^+$ ion is not part of the more general $(n\text{M+H})^+$ decay sequence but the $C_4H_9O_2^+$ ion is.

One of the most interesting findings from the fragmentation of secondary ions from PMMA is that the most commonly lost neutral fragments are CO and CH_xO, where $x = 4$ is usual. This is easily interpreted as the loss of pendant methyl ester groups and is supported by the observation that these losses often coincide, with the loss of CH_xO prior to the loss of CO. The loss of side groups to explain the secondary ions observed in SIMS of poly(methacrylates) is a well established argument [14]. This study demonstrates that such losses occur during the flight of ions in ToF-SIMS and are usually the result of a two-step process. A possible mechanism is illustrated in Scheme 5.

The fragmentation of secondary ions in PTFE is interesting, the predominant neutral loss from high mass ions appears to be the difluorocarbene unit. This may be taken as an indication of the retention of polymer structure in the ion, but may also be a consequence of the ease of formation of the difluorocarbene diradical. A comparison with other perfluorinated polymers, such as poly(hexafluoropropene) would be useful to distinguish these effects. The saturated secondary ions, $C_6F_{11}^+$ and $C_5F_9^+$, also fragment with loss of a single tetrafluoroethylene unit and this may be taken as evidence of the linear structure of these ions. The results found here are in excellent agreement with a collisionally activated dissociation (CAD) study using a tandem quadrupole analyser [15]. CAD permits the fragmentation of ions to be studied in a selective manner and without the requirement for a fortuitous metastable decay process. Unfortunately, for virtually all ToF-SIMS instruments it is not possible to conduct CAD experiments. The analysis of metastable ions in the manner described in this paper to obtain additional structural information is of great benefit to the ToF-SIMS analytical community who do not have access to specialised CAD instrumentation.

6. Conclusions

A simple method to determine the parent and daughter masses of metastable ions observed in a single stage reflectron time-of-flight detector has been described. The method is similar to our previous approach [1], but has the convenience of using the apparent mass of the metastable ion. This analysis provides metastable decay pathways that are a powerful tool for analysts to identify metastable ions and use these to interpret molecular structure and identify complicated molecules. It should be noted that we have demonstrated the method on homogeneous, known materials and further work on mixed and unknown materials is required to validate its utility. This approach is complementary

to G-SIMS, and in particular, G-SIMS fragmentation pathway mapping [16,17] (G-SIMS-FPM) which allows the molecular structure to be inferred by identifying the linkage between structurally significant fragment ions. Metastable analysis may be employed to confirm the structural links suggested by G-SIMS-FPM, or to confirm links in cases of ambiguity, such as in mixed systems. G-SIMS requires the use of two different primary ion sources, which are not available on all instruments. Metastable analysis, however, does not require additional primary ion sources and may be used to infer structurally important ions from the metastable decay pathways. We have demonstrated the origin of metastable peak shapes and highlighted that the analysis of these shapes in terms of the kinetic energy release and kinetics is possible, but not straightforward. Finally, we have undertaken a comprehensive survey of metastable ions observed in the ToF-SIMS spectra of four important polymers and demonstrated the additional structural insight that this analysis can provide.

Acknowledgement

This work forms part of the chemical and biological knowledge base programme of the National Measurement System of the UK Department of Innovation, Universities and Skills.

References

[1] I.S. Gilmore, M.P. Seah, Appl. Surf. Sci. 144–145 (1999) 26.
[2] J.M. L'Hermite, L. Marcou, F. Rabilloud, P. Labastie, Rev. Scientific Inst. 71 (2000) 2033.
[3] X. Tang, R. Beavis, W. Ens, F. LaFortune, B. Schueler, K.G. Standing, Int. J. Mass Spectrom. Ion Processes 85 (1988) 43.
[4] X. Tang, W. Ens, K.G. Standing, J.B. Westmore, Anal. Chem. 60 (1988) 1791.
[5] D.F. Barofsky, G. Brinkmalm, P. Hakansson, B.U.R. Sundqvist, Int. J. Mass Spectrom. Ion Processes 131 (1994) 283.
[6] C.R. Ponciano, E.F. da Silviera, J. Phys. Chem. A 106 (2002) 10139.
[7] A.G. Shard, C. Volland, M.C. Davies, T. Kissel, Macromolecules 29 (1996) 748.
[8] I.S. Gilmore, M.P. Seah, Appl. Surf. Sci. 161 (2000) 465.
[9] I.S. Gilmore, M.P. Seah, Appl. Surf. Sci. 203–204 (2003) 551.
[10] I.S. Gilmore, M.P. Seah, Appl. Surf. Sci. 231–232 (2004) 224.
[11] I.S. Gilmore, M.P. Seah, F.M. Green, Surf. Interface Anal. 37 (2005) 651.
[12] A.G. Shard, M.C. Davies, E. Schacht, Surf. Interface Anal. 24 (1996) 787.
[13] R. Ogaki, F.M. Green, I.S. Gilmore, A.G. Shard, S. Luk, M.R. Alexander, M.C. Davies, Surf. Interface Anal. 39 (2007) 852.
[14] M.J. Hearn, D. Briggs, Surf. Interface Anal. 11 (1988) 198.
[15] G.J. Leggett, D. Briggs, J.C. Vickerman, J. Chem. Soc. Faraday Trans. 86 (1990) 1863.
[16] I.S. Gilmore, F.M. Green, M.P. Seah, Appl. Surf. Sci. 252 (2006) 6601.
[17] F.M. Green, E.A. Dell, I.S. Gilmore, M.P. Seah, Int. J. Mass Spectrom., in preparation.